Advanced Commercial Power System Protection Practices Applied to Naval Medium Voltage Power Systems

David Whitehead and Normann Fischer
Schweitzer Engineering Laboratories, Inc.

Revised edition released August 2008

Originally presented at the
IEEE Electric Ship Technologies Symposium, July 2005

Advanced Commercial Power System Protection Practices Applied to Naval Medium Voltage Power Systems

David Whitehead, *Senior Member*, *IEEE*, and Normann Fischer

***Abstract*— In the U.S. Navy's transition to an all-electric ship, system designers must take great care to ensure that critical design choices provide highly reliable and safe power system operation and protection during all mission scenarios. Transitioning from low voltage (450 V_{AC}) radial configurations to medium voltage (13.8 kV_{AC}) multi-source systems requires new naval protection schemes. This paper specifically analyzes methods for quickly determining ground faults in ungrounded and high-impedance grounded naval power systems.**

***Index Terms*— Fault Location, Grounding, Power System Protection, Relays.**

I. Introduction

Traditional naval power systems generally consist of 450 V_{AC} generators, bus-ties, switchboards with circuit breakers, and loads arranged in a radial, ungrounded configuration. Naval power systems are transforming into multisource or looped power systems that consist of multiple power sources and multiple paths to serve electrical loads. These configurations provide system designers greater flexibility managing generation versus load requirements, but at the cost of more complicated protection schemes.

Ungrounded power systems allow power systems to continue operation with an uncleared single-phase-to-ground fault. However, a second phase-to-ground fault on a different phase presents the system with a phase-to-phase fault. These phase-to-phase faults are almost always associated with high magnitude current values. Thus, the first phase-to-ground fault should be quickly identified or isolated so that another fault does not result in further degradation to system reliability. This paper describes two methods for determining phase-to-ground faults in ungrounded naval power systems.

II. Background

Naval power systems are unique compared to most traditional terrestrial power systems because they are designed to operate in an ungrounded or very high impedance grounded configuration. The latter systems operate the same as an ungrounded system if the system loses its grounding point or if the grounding impedance is very high. In an ungrounded power system there is no intentional connection to ground and loads are connected phase-to-phase. Fig. 1 shows a single-line diagram for an ungrounded power system.

D. Whitehead is with Schweitzer Engineering Laboratories, Inc. Pullman, WA 99163 USA (e-mail: david_whitehead@selgs.com).

N. Fischer is with Schweitzer Engineering Laboratories, Inc. Pullman, WA 99163 USA (e-mail: normann_fischer@selinc.com).

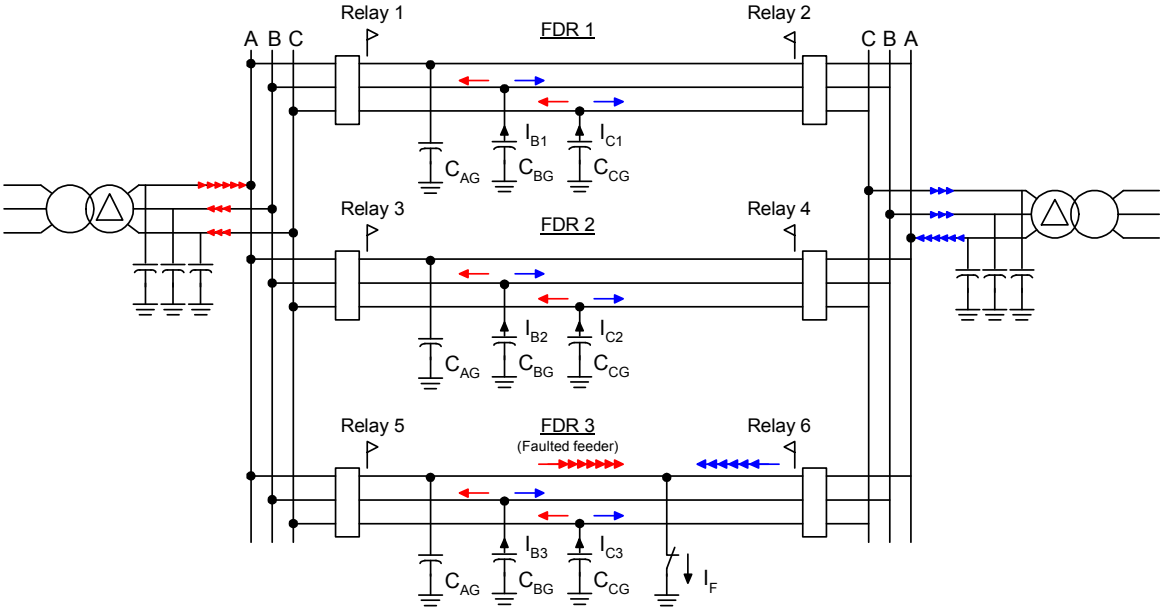

Fig. 1 Example Ungrounded System Single-Line Diagram

The single greatest advantage of an ungrounded power system is that for a single-phase-to-ground (SLG) fault the voltage triangle remains intact and therefore loads can remain in service. When a SLG fault occurs, the faulted phase potential decreases to near zero while the healthy phase magnitudes increase by a factor of 1.73 and shift 30 degrees toward one another. At the same time, the zero-sequence voltage increases to three times the normal phase-to-neutral voltage. Fig. 2 demonstrates these two conditions. Fig. 2(a) shows an unfaulted ungrounded system. Fig. 2(b) shows how the voltage triangle shifts relative to ground for an A-to-ground fault [1].

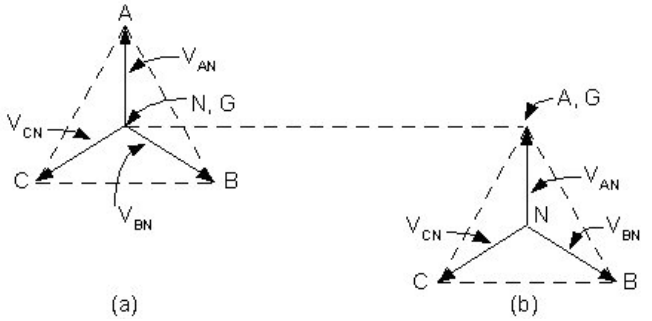

Fig. 2 Voltage Triangle Remains Intact for SLG Faults

In a balanced, unfaulted system the residual current for the protected line is zero ($3I_{0L} = 0$). For this state, the system neutral (N) is at ground potential ($V_{NG} = 0$) (see Figure 2a). Natural system asymmetry produces a small amount of neutral current and shifts the system neutral from the ideal ground potential of $V_{NG} = 0$. However, the amount of shift is so small that we can ignore this point in this discussion. For a solid A-to-ground fault ($R_F = 0$), the phase-to-ground voltage of the two remaining unfaulted phases equals the phase-to-phase voltage ($V_{BG} = V_{BA}$, $V_{CG} = V_{CA}$) and the neutral-to-ground voltage equals the negative of the source phase-to-neutral voltage corresponding to the faulted phase ($V_{NG} = - V_{AN}$).

The traditional method for locating single-phase-to-ground faults was to disconnect a feeder and determine whether the zero-sequence voltage decreased to its prefault value. If the zero-sequence voltage returned to its prefault value after the feeder was disconnected, the operator deduced that it was the faulted section

This elimination method is very time consuming and unnecessarily interrupts loads or causes extra switchings. By analyzing both phase-domain and symmetrical component models, we have derived methods for determining the faulted phase using measured ac signals.

A. Single-Ended Phase-to-Ground Fault Detection in Ungrounded Power Systems

Referring back to Fig. 1, with a fault placed between Relay 5 and Relay 6, we can analyze the resulting relationship between the voltage and current from the perspective of these two devices. Fig. 3 shows the phase-angle relationship between the current flowing in and to the fault and the phase voltages during the fault. Note that in this figure the fault currents flowing in the unfaulted phases (I_{B1} ...I_{C3}) lead the associated unfaulted phase voltages (V_{BG} and V_{CG}) by 90 degrees during the fault (i.e., I_{B1}, I_{B2}, and I_{B3} lead V_{BG} by 90 degrees). Note, too, that the fault current (I_F) can be calculated as:

$$I_F := -(I_{B1} + I_{B2} + I_{B3} + I_{C1} + I_{C2} + I_{C3}) \quad (1)$$

The magnitude of the fault currents (I_{B1}, I_{B2}, etc.) flowing in the unfaulted phases depends on the line-to-ground capacitance of the unfaulted phases. Smaller unfaulted-phase line-to-ground capacitive reactance (or larger susceptance), results in larger phase-fault currents. Therefore, the magnitude of the fault current flowing in the faulted feeder is dependent on the susceptance of the ungrounded power system, if we ignore the fault resistance [2].

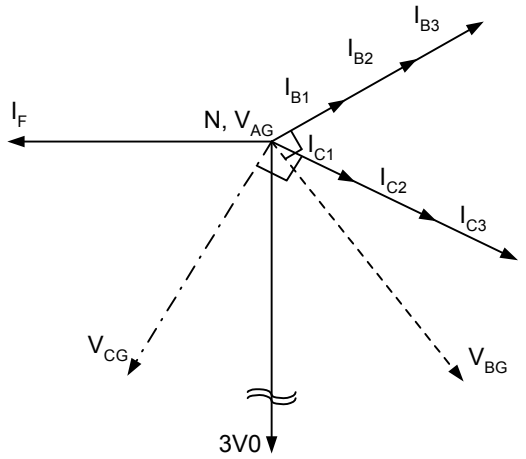

Fig. 3 A-Phase-to-Ground Fault on Feeder 3

Fig. 4 shows the phasor diagram of Fig. 3 broken up into two phasor diagrams: one for the faulted feeder and one for the unfaulted feeders.

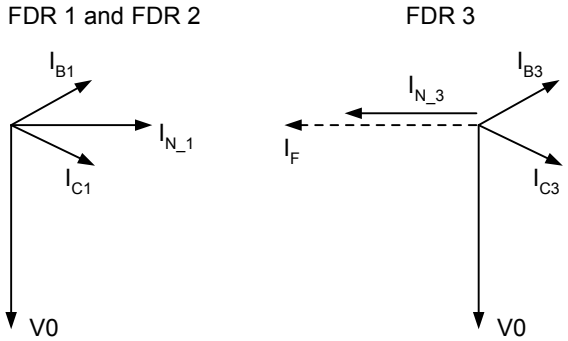

Fig. 4 Unfaulted and Faulted Feeder Phasor Diagram

Analysis of the phasor diagram in Fig. 4a shows that the residual current (I_{N_1}) leads the residual voltage (V0) by 90 degrees, while for the faulted feeder (Fig. 4b) the residual current lags the residual voltage by 90 degrees. Also note that in Fig. 4 the residual current (I_N) measured by each relay is less than the total fault current (I_F). The residual current (I_{N_3}) is lower than the fault current (I_F) by an amount that can be expressed by Equation 2. This is because the line-to-ground capacitance of the faulted feeder is actually reducing the calculated zero-sequence current.

$$I_{N\_3} := I_F - (I_{B3} + I_{C3}) \quad (2)$$

From this simple analysis of the phasor diagrams in Fig. 4, we can conclude that detecting the faulted feeder in an ungrounded network requires determining whether the residual current is leading or lagging the residual voltage. If the residual current is leading the residual voltage, the fault is behind the feeder and the feeder is unfaulted. If the residual current lags the residual voltage, then the fault is on the feeder. So by simply measuring and calculating the phasor relationship between the residual voltage and residual current, we can then identify the faulted feeder on an ungrounded power system.

The residual voltages and currents represent the zero-sequence voltage and currents, respectively. Fig. 5 shows the sequence connection diagram of the fault scenario shown in Fig. 1 [3]. Note that we are omitting the shunt conductance (G) in the sequences diagram. These values are typically an order of magnitude greater than the susceptance (B) values and omitting them does not significantly detract from the accuracy of our analysis.

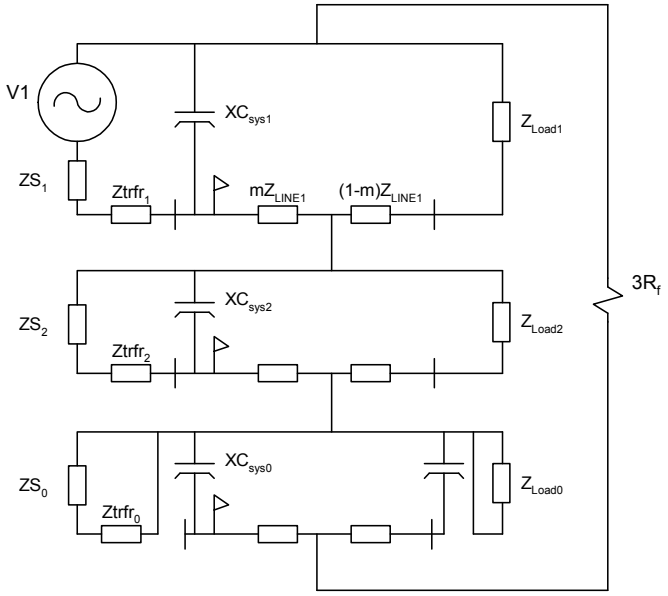

Fig. 5 Sequence Connection Diagram for A-Phase-to-Ground Fault on a Radial System With Load

If we consider the following, we can further reduce the diagram in Fig. 5:

- The impedance of XC_{sys1} is much greater (in the order of 100 times) than the sum of ZS_1 and $Ztrfr_1$ [$XC_{sys1} >> ZS_1+Ztrfr_1$]. Thus, we can ignore the effect of XC_{sys1} and consider it infinite.
- The impedance of XC_{sys2} is much greater than the sum of ZS_2 and $Ztrfr_2$. Thus, we can ignore the effect of XC_{sys2} and consider it infinite.
- The impedance XC_{sys0} is much greater than the sum of ZS_1, ZS_2, $Ztrfr_1$ and $Ztrfr_2$, [$XC_{sys0} >> ZS_1 + ZS_1 + Ztrfr_1 + Ztrfr_1$]. We cannot ignore this impedance because this impedance is in series with the positive- and negative-sequence impedances.

Based on the above considerations, we can now reduce the sequence diagram of Fig. 5 to that of Fig. 6. Looking at Fig. 6, note that the dominant impedances for a SLG fault are the zero-sequence capacitance of the power system and the fault resistance R_f.

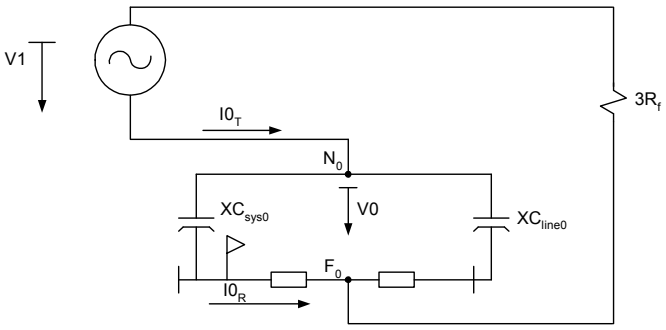

Fig. 6 Reduced Sequence Connection Diagram for A-Phase-to-Ground Fault on a Radial System With Load

The impedance connection shown in Fig. 6 confirms our analysis of the single-line-to-ground fault in the phase domain. How can we use the sequence domain to identify the faulted phase? The answer is to use the A-phase voltage as the reference phase for the positive-sequence voltage and then derive the equivalent sequence diagrams for B- and C-phase-to-ground faults.

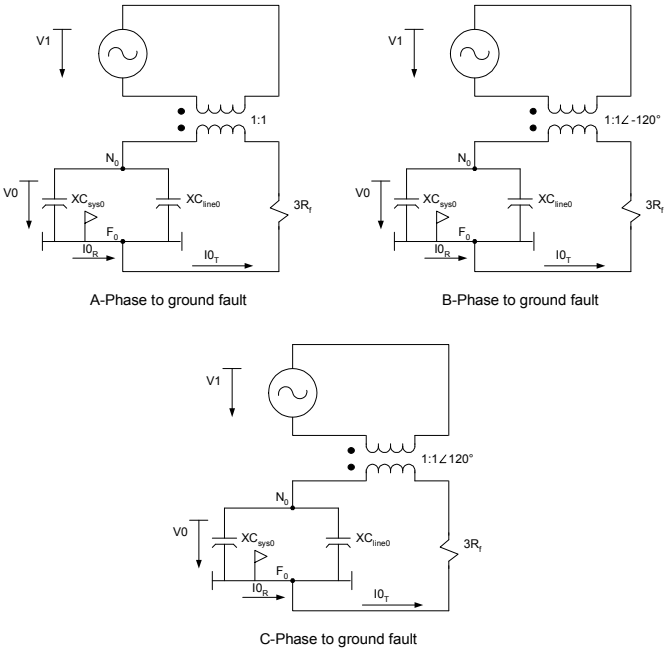

Fig. 7 Reduced Sequence Connection Diagram for A-, B-, and C-Phase-to-Ground Faults on a Radial System With Load

If we assume a $R_f = 0\ \Omega$, and use the sequence diagram of Fig. 7, we can draw the phasor diagram showing the relationship between the positive-sequence voltage and the zero-sequence current (I0), as is shown in Fig. 8.

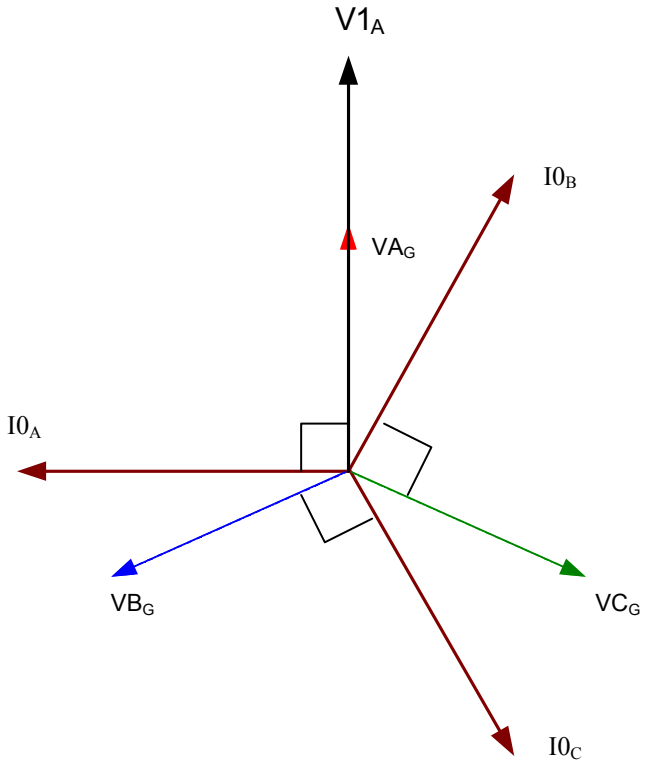

Fig. 8 Relationship Between the Positive-Sequence Voltage and Zero-Sequence Current

Extending our earlier observations on fault direction, we can observe the following from Fig. 8, using only the angular relationship between the positive-sequence voltage ($V1_A$) and the zero-sequence current (I0).

- A-Phase-to-ground fault if I0 leads $V1_A$ by 90 degrees.
- B-Phase-to-ground fault if I0 lags $V1_A$ by 30 degrees.
- C-Phase-to-ground fault if I0 lags $V1_A$ by 150 degrees.

If we do not ignore the system conductance, the resulting angle between V0 and I0 is a value smaller than 90 degrees. For example, assume that the ratio of susceptance (jB) to conductance (G) is 20 to 1 (typically the value is larger than this and in the order of 100:1). For this example, the resulting angle between V0 and I0 would be arctan (20) = 87.14°. Increasing the ratio only moves the resulting angle more towards 90 degrees.

By comparing the zero-sequence current angle to that of positive-sequence voltage, we can determine the faulted phase. However, consider what happens if the fault resistance (R_f) is not zero. Also, what happens if the fault resistance is equal to or greater than the system line-to-ground capacitance ($|R_f| > |XC_{line\_0}|$)?

To answer these questions, let us examine the result of increasing the fault resistance for an A-phase-to-ground fault. Fig. 9 represents a scenario of three different fault resistances:

1. $R_f << XC_{line\_0}$
2. $R_f = 1/3\ XC_{line\_0}$
3. $R_f >> XC_{line\_0}$

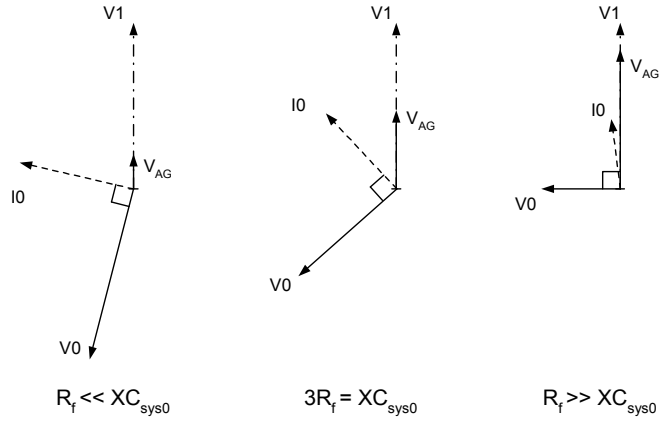

Fig. 9 Effect of Fault Resistance on Zero-Sequence Current to Positive-Sequence Voltage Angle

From the three phasor diagrams of Fig. 9, you can see that increasing the fault resistance decreases the angle between the zero-sequence current and positive-sequence voltage referenced to the faulted phase. Using this observation and applying it to the B- and C-phase-to-ground faults, we can create the phasor diagram shown in Fig. 10.

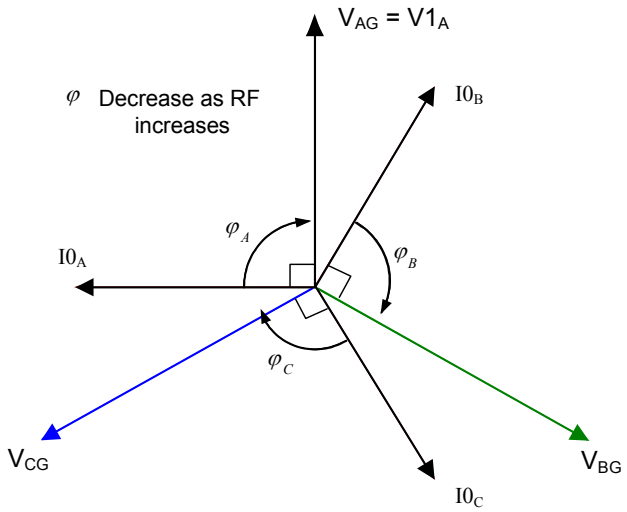

Fig. 10 Phasor Diagram Relationship of $V1_A$ versus $I0_A$, $I0_B$, and $I0_C$

Using the information obtained from Fig. 9 and Fig. 10, it is now possible to generate a phase-to-ground fault diagram, as shown in Fig. 11.

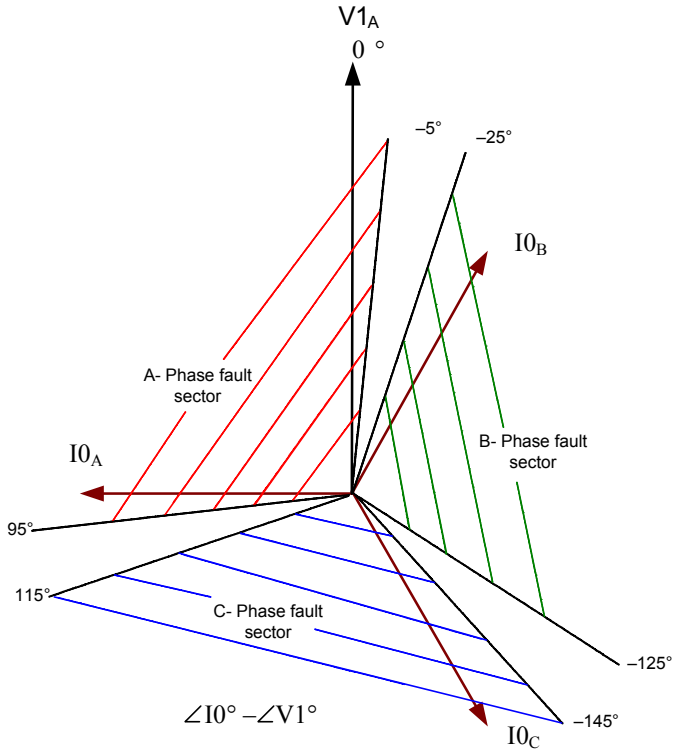

Fig. 11 Zero-Sequence Faulted Sectors Relative to $V1_A$

B. Double Ended Phase-to-Ground Fault Detection in Ungrounded Power Systems

Work by J. Roberts, H. Altuve, and D. Hou describes a zero-sequence directional element for radial lines [4]. The authors describe a method for determining forward or reverse faults based on a resulting impedance calculation used in solidly grounded power systems; see Equation 3:

$$z0 = \frac{\mathrm{Re}\left[3V0 \cdot (3I_0 \cdot 1\angle ZL_0\_Ang)^*\right]}{\left|3I_0\right|^2} \quad (3)$$

Where:

3V0	=	Summation of phase voltages ($V_A + V_B + V_C$)
$3I_0$	=	Summation of phase currents ($I_A + I_B + I_C$)
ZL_0_Ang	=	Zero-seq. line impedance angle
Re	=	Real operator
*	=	Complex conjugate

If the resulting z0 calculation is negative, the fault is forward. If the resulting calculation is positive, the fault is reverse.

This directional element is useful for applications with large amounts of zero-sequence currents available to reliably perform protection. However, in ungrounded systems the zero-sequence fault current available to a single measuring relay may be quite small for remote faults. Modern high-speed line current differential relays use communication channels to exchange current information measured at line ends [5]. Thus, each line-end relay has the total current flowing into and out of a line. For example, in Fig. 1, Relays 1 and 2 exchange current measurements, as do Relays 3 and 4, and Relays 5 and 6. By taking advantage of the communication channel, we can improve the sensitivity of a new zero-sequence impedance directional protection element for detecting and isolating ground faults in an ungrounded or high-impedance grounded power system.

Reconsider the three-feeder power system section in Fig. 1. Fig. 12 shows the zero-sequence network with an A-phase-to-ground fault at the middle of Feeder 3. Each feeder line in Fig. 12 is represented with a pie-section model. In Fig. 12 we omitted the generator terminal capacitances for illustrative clarity.

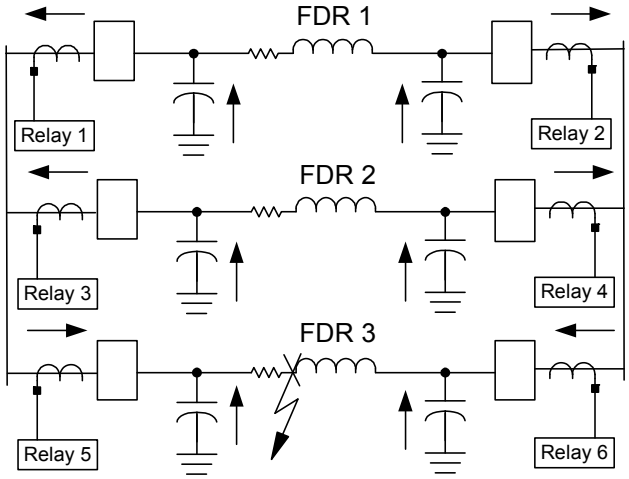

Fig. 12 Zero-Sequence Network With an A-Ground

Measuring the zero-sequence current at each relay allows us to note the following:

- $3I_0$ measured by Relays 5 and 6 have equal magnitude and are in-phase.
- $3I_0$ measured by Relays 1, 2, 3, and 4 are in-phase for the out-of-section fault, but nearly 180 degrees out-of-phase with the $3I_0$ measured by the relays on the faulted line.

The 3I0 current is equal at each end of Line 3 because the ground fault on Line 3 is exactly at mid span (i.e., m – 0.5) and the lines are bussed together at each line end. The last observation confirms that the zero-sequence capacitance from Feeders 1 and 2 acts as a fault source.

The zero-sequence current measured by the relays associated with the faulted feeder, Relays 5 and 6, is shown in Fig. 13, with current flowing out of the bus.

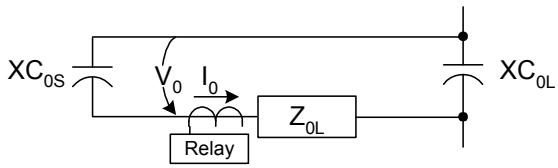

Fig. 13 Zero-Sequence Network for the Forward Ground Fault

However, Relays 1, 2, 3, and 4 measure current flowing into the bus as shown in Fig. 14.

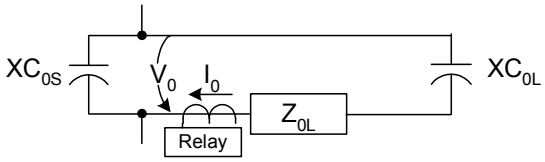

Fig. 14 Zero-Sequence Network for the Reverse Ground Fault

Let us next analyze the direction of the zero-sequence current for Relays 1 and 2. Notice that these currents have the same direction relative to the zero-sequence bus voltage(s). We can vectorially add the two current measurements, using the communication link between Relays 1 and 2, to produce a current that has a magnitude twice that measured by either line-end relay. To quantify the algorithm shown by Equation 4, we can expand each of the zero-sequence current terms as follows:

$$z0T = \frac{\mathrm{Re}\left[3V0 \cdot \left((3I_{NL} + 3I_{NR}) \cdot 1\angle ZL_0\_Ang\right)^*\right]}{\left|(3I_{NL} + 3I_{NR})\right|^2} \quad (4)$$

Where:

- 3V0 = Summation of phase voltages ($V_A + V_B + V_C$)
- $3I_{NL}$ = Zero-seq. current measured by the local relay
- $3I_{NR}$ = Zero-seq. current measured by the remote relay
- ZL_0_Ang = Zero-seq. line impedance angle
- Re = Real operator
- * = Complex conjugate

Equation 4 produces a resulting plot on the zero-sequence impedance plane, as shown in Fig. 15. If the resulting impedance calculation is below the forward threshold (and all of the supervisory conditionals are met), the fault is declared forward. Conversely, if the measured impedance is above the reverse threshold, the fault is declared reverse.

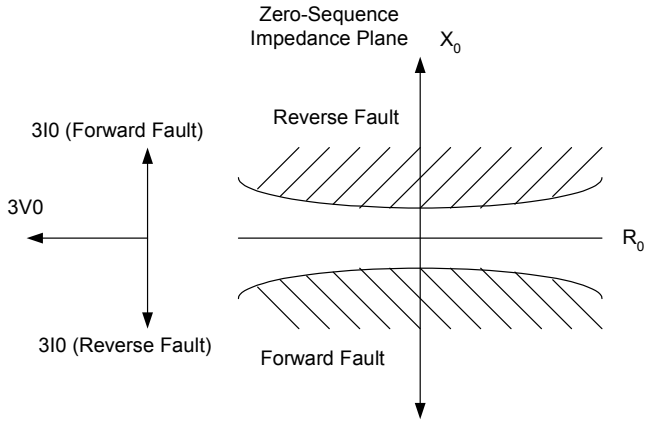

a. Zero-Seq. Phasors

b. Impedance-Plane Directional Element Characteristics

Fig. 15 Ground Directional Element Characteristics

To examine the relationship of zero-sequence voltage and current for the simple three-line system discussed above, we modeled a system of three 800-meter long, 400 MCM cables connected to two buses in the ungrounded system shown in Figure 1. The power system is operating at 4.16 kV_{AC}. For a mid-line fault on Feeder 3, the relays make the following measurements (secondary), as shown in Table 1:

TABLE 1
FEEDER 3 MID-LINE FAULT

Relay	3V0 (V)	3I0_L (mA)	3I0_R (mA)
Relay 1	207∠180°	2.5∠-90°	2.5∠-90°
Relay 2	207∠180°	2.5∠-90°	2.5∠-90°
Relay 3	207∠180°	2.5∠-90°	2.5∠-90°
Relay 4	207∠180°	2.5∠-90°	2.5∠-90°
Relay 5	207∠180°	5∠90°	5∠90°
Relay 6	207∠180°	5∠90°	5∠90°

Assuming a totally capacitive zero-sequence line angle, the resulting total zero-sequence calculation (z0T) for each relay is shown in Table 2:

TABLE 2
FEEDER 3 MID-LINE FAULT IMPEDANCE CALCULATIONS

Relay	Z0_Total	Direction
Relay 1	41,400 Ω	Reverse
Relay 2	41,400 Ω	Reverse
Relay 3	41,400 Ω	Reverse
Relay 4	41,400 Ω	Reverse
Relay 5	-20,700 Ω	Forward
Relay 6	-20,700 Ω	Forward

As we can see, Relays 5 and 6 correctly identify Feeder 3 as the faulted apparatus, while Relays 1, 2, 3, and 4 restrain from making a forward declaration.

Now let us place the same fault closer to Relay 2. This results in a larger zero-sequence current measured by Relay 1, but a smaller current measured by Relay 2. In this case, Relay 2 may not measure enough zero-sequence current to reliably make a fault determination using single-ended methods alone. However, because the zero-sequence currents from each line end are vectorially added, both relays can reliably make a fault determination.

III. CONCLUSION

This paper discusses two new methods for ground fault detection in ungrounded or high-impedance-grounded systems. These results are highly applicable to naval power systems. The first method analyzes the relationship between the positive-sequence voltage and zero-sequence current phase angle to determine the faulted phase. The second method uses the zero-sequence voltage and local and remote zero-sequence currents to determine zero-sequence impedance.

Follow-up papers will discuss high-speed reconfiguration methodologies using these ground fault detection methods.

IV. REFERENCES

[1] J.B. Roberts and D. Whitehead, "Ground Fault Detection System for Ungrounded Power Systems," U.S. Patent 6 785 105, Aug. 31, 2004.

[2] N. Fischer and M. Feltis, "Applying the SEL-351 Relay to an Ungrounded System," Schweitzer Engineering Laboratories, Inc. [Online]. Available: http://www.selinc.com/ag02xx.htm (select #AG2002-06).

[3] J. L. Blackburn, *Protective Relaying, Principles, and Applications*, 2nd ed. New York: Marcel Dekker, 1998, pp. 190-195.

[4] J. Roberts, H. Altuve, and D. Hou, "Review of Ground Fault Protection Methods for Grounded, Ungrounded, and Compensated Distribution Systems," in *2001 28th Annual Western Protective Relay Conference Proceedings*, p. 10.

[5] J. Roberts, D. Tziouvaras, and G. Benmouyal, "The Effect of Multiprinciple Line Protection on Dependability and Security," in *54th Annual Conference for Protective Relay Engineers*, College Station, Texas, April 3-5, 2001.

V. BIOGRAPHIES

David Whitehead, P.E. is the Chief Engineer, GSD Division, and a Principal Research Engineer for Schweitzer Engineering Laboratories. Prior to joining SEL he worked for General Dynamics, Electric Boat Division as a Combat Systems Engineer. He received his BSEE from Washington State University in 1989 and his MSEE from Rensselaer Polytechnic Institute in 1994. He is a registered Professional Engineer in Washington State and Senior Member of the IEEE. Mr. Whitehead holds six patents with several others pending. He designs and manages the design of advanced hardware, embedded firmware, and PC software.

Normann Fischer joined Eskom as a Protection Technician in 1984. He received a Higher Diploma in Technology, with honors, from the Witwatersrand Technikon, Johannesburg, in 1988 and a B.Sc. in Electrical Engineering, with honors, from the University of Cape Town in 1993. A member of the South Africa Institute of Electrical Engineers, he was a Senior Design Engineer in Eskom's Protection Design Department for three years, then joined IST Energy as a Senior Design Engineer in 1996. In 1999, he joined Schweitzer Engineering Laboratories as a Power Engineer in the Research and Development Division.

VI. PREVIOUS PUBLICATIONS

Presented at IEEE Electric Ship Technologies Symposium (ESTS 2005)